THE JOURNAL OF PHYSICAL CHEMISTRY C
A JOURNAL OF THE AMERICAN CHEMICAL SOCIETY

pubs.acs.org/JPCC

Article

Silylethynyl Substitution for Preventing Aggregate Formation in Perylene Diimides

Erkan Aksoy,* Andrew Danos, Chunyong Li, Andrew P. Monkman,* and Canan Varlikli

Cite This: *J. Phys. Chem. C* 2021, 125, 13041−13049

Read Online

ACCESS | Metrics & More | Article Recommendations | Supporting Information

ABSTRACT: Ethynylene-bridged perylene diimides (PDIs) with different sized silane groups have been synthesized as a steric blocking group to prevent the formation of non-radiative trap sites, for example, strong H-aggregates and other dimers or excimers. Excited singlet-state exciton dynamics were investigated by time-resolved photoluminescence and ultrafast pump−probe transient absorption spectroscopy. The spectra of the excimer or dimer aggregates formed by the PDIs at high concentrations were also determined. Although the photophysical properties of the bare and shielded PDIs are identical at micromolar concentrations, more shielded PDI2 and PDI3 exhibited resistance to aggregation, retaining higher photoluminescence quantum yield even at 10 mM concentration and in neat films. The PDIs also exhibited high photostability (1 h of continuous excitation), as well as electrochemical stability (multiple cycles with cyclic voltammetry). Prevention of dimer/aggregate formation in this manner will extend the uses of PDIs to a variety of high concentration photonics and optoelectronic applications, such as organic light-emitting diodes, organic photovoltaics, and luminescent solar concentrators.

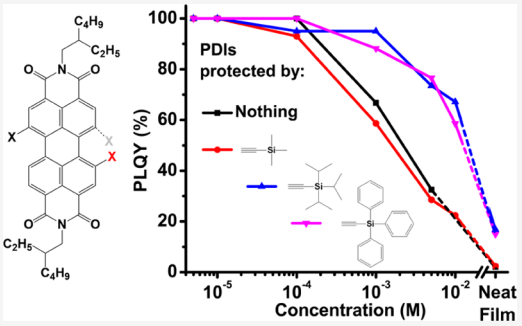

INTRODUCTION

Perylene diimides (PDIs) are one of the important chromophore groups, with extended π-conjugation systems leading to many optical and optoelectronic applications. Of particular usefulness in applications are their high absorption coefficients ($\varepsilon > 10^4$ M^{-1} cm^{-1}) in the visible region, strong electron affinities, high electron mobilities, and photoluminescence quantum yields (PLQYs or Φ, typically near 100%). PDIs also frequently exhibit excellent optical, thermal, and electronic stability.[1−7] Combined with their n-type charge transport characteristics and singlet emission, PDIs are commonly applied in organic or perovskite solar cells, organic light-emitting diodes (OLEDs), and organic transistors.[8−13] Due to their large and chemically tuneable ε in the blue-green region (400−550 nm), they can also be used to obtain white light with downconverters[4,14,15] for lighting applications or in organic luminescent solar concentrators[16−18] for hybrid photonic devices.

The superior optical properties of PDIs and other flat polycyclic aromatic hydrocarbon molecules in solution phase are often not preserved in films due to aggregation-caused quenching (ACQ).[19,20] The same is also true for regular perylenes,[21] which are often used as blue emitters and for triplet−triplet annihilation applications.[22,23] The transitions associated with the lowest energy excitonic states are critical to the performance of organic photonic devices,[19,24,25] with deactivation and quenching by dimer[26,27] or excimer[28,29] states able to outcompete many desired processes—such as charge transfer and transport,[30] exciton diffusion,[31] and intersystem crossing.[26,27,32] PDIs that form such excimer, dimer, or aggregate states also often exhibit significantly different photophysical properties compared to isolated molecules, making understanding and developing device applications complicated at higher concentrations.[33] For example, red-shifted photoluminescence (PL) spectrum, increased fluorescence lifetime, and losses in PLQYs are all commonly reported.[19,34−36] The deleterious effects of high-concentration multimolecular interactions and ACQ are further amplified in systems where dyes are anchored at high loading onto nanoparticle[28] surfaces as ligands, with such dye-particle composite materials generating strong interest for light-harvesting and photon conversion applications.[37,38]

Avoiding the formation of these quenching states is therefore important for improving the performance of PDI devices, with several molecular design strategies already reported toward protecting this and other optically active cores from interactions with neighboring molecules.[1,39−44] One of the popular strategies for preventing $\pi-\pi$ aggregations of PDIs is to modify the bay positions with large steric groups, such as *tert*-butylphenoxy.[16,31,44−49] This approach can either

Received: April 7, 2021
Revised: May 19, 2021
Published: June 2, 2021

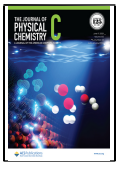

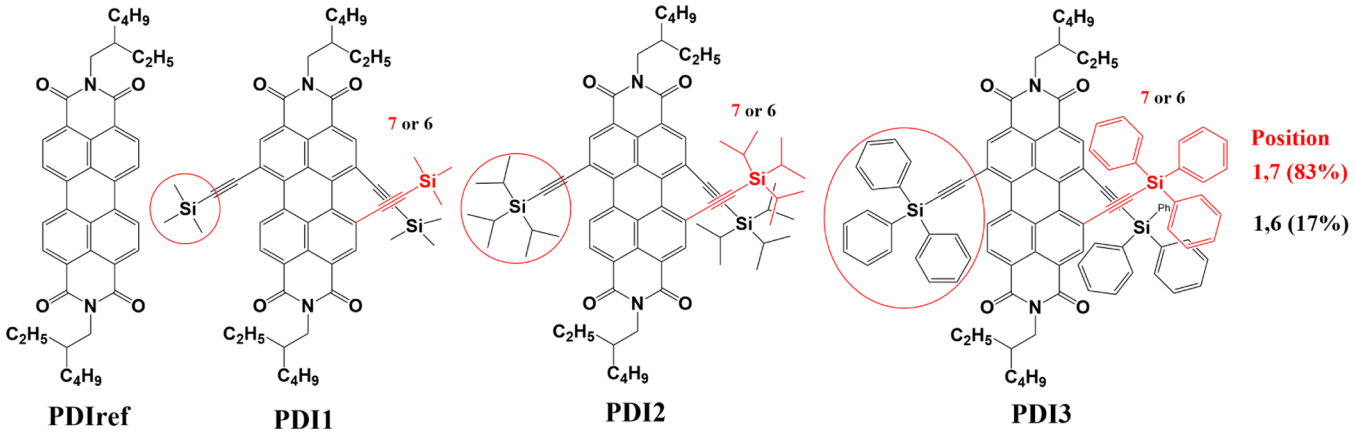

Figure 1. Synthesized perylene derivatives.

directly block the approach of neighboring molecules or twist the backbone of the PDI making it less planar and therefore also less susceptible to π-stacking interactions.[46] In recent studies, this approach has been shown to preserve excellent PLQY values upward of 90% in crystals[44] and 60% in neat films.[49] However, as the linking ether bridges do not fully isolate the PDI core from the electronic system of the shielding groups, this strategy also introduces slight changes in the absorption and emission spectra of the sterically shielded materials even in dilute solutions. Indeed, the degree of spectral redshift increases with the size of the shielding groups,[49] while in other systems, these groups can directly interact with the PDI core to form charge-transfer states[48] or influence electron transport properties.[50] Elsewhere, fused systems can lengthen the π-conjugation system without causing the PDIs to twist, which facilitates exciton diffusion and improves charge transport.[50,51] The redshifting effect of increased bay substituent bulk is not as pronounced in similar studies of imide-substituted PDIs though,[1] indicating different levels of electronic communication through that site.

Inspired by the electronically insulating properties of silyl-containing spacer materials in thermally activated delayed fluorescence exciplex blends,[52,53] in this study, a reference PDI (PDIref) and three bay-substituted ethynyl-bridged PDIs (PDI1, PDI2, and PDI3) with bulky silane groups were synthesized (Figure 1) and their exciton dynamics investigated at high and low concentrations. Sonogashira coupling of acetylene-bridged derivatives with the sp hybrid structure to the bay positions of the PDI[4,54,55] is found to expand the electronic system of the PDI core, although the high PLQY in dilute solution is preserved.[4,56] Crucially, no further spectral changes are observed as the bulk of the shielding groups varied beyond the silicon atom.

At higher concentrations, complicated dynamics involving excimer and higher-order aggregate states were revealed in the PDIs using time-resolved spectroscopy. The excited-state properties of PDIs were also compared by fs-transient absorption spectroscopy (TAS) and PLQY measurements at different concentrations. The extent of PDI interactions and ACQ decreased as the silane steric size increased from PDI1 to PDI2 but with no additional protecting effect as it was further increased from PDI2 to PDI3.

METHODS

Full description of all synthetic methods, and structural, electrochemical, and optical characterization methods are included in the Supporting Information.

RESULTS AND DISCUSSION

Synthesis. Previously reported PDIref[57] was used as a reference in this study due to its planar aromatic structure and its predisposition to form molecular interactions. In order to compare with shielded PDIs modified with different volumes of steric groups, previously reported PDI2[56] as well as newly prepared PDIs 1 and 3 were synthesized (Figure S1) following the Sonogashira coupling synthetic process in the literature.[56,58] The new materials PDI1 and PDI3 were additionally characterized by NMR and high-resolution mass spectroscopy.

The first of the two most well-known examples of these regioisomer synthesis methods starts with the synthesis of perylenetetraester (PTE) and dibromoperylenetraester (DBrPTE) and then conversion of the 1,7-isomeric DBrPTEs obtained by crystallization of the mixed-isomer 1,6 and 1,7-DBrPTE derivatives to 1,7-dibromoperylenetetracarboxylic-dianhydride (DBrPTCDA).[59,60] In the second method, 1,6 and 1,7-regio isomers of diBrPDIs are synthesized from specific alkyl-amine derivatives and purified by column chromatography. The purified 1,6 or 1,7-DBrPDI derivatives are then hydrolyzed in basic medium and converted back into the DBrPTCDA derivatives. The target regioisomer is then obtained by the re-imidization reaction with the desired functional group.[61,62] However, the reaction conditions provided here to obtain 1,6 and 1,7 acetylenyl-bonded PDI2 may guide researchers wishing to synthesize the individual isomers (to obtain isomer purity acetylene bridges or fused systems[63]) without needing to separate a mixture. It is quite efficient to subsequently remove the silane groups under basic reaction conditions.

First, brominated PDIs of 1,7-func. (87% isomeric purity, the remainder being 1,6 brominated) were prepared[56] and degassed in triisopropylamine (base medium) to remove oxygen. Then, $[Pd(PPh_3)_4]$ and CuI catalysts and acetylene sources [(trimethylsilyl)acetylene for PDI1, (triisopropylsilyl)-acetylene for PDI2 and (triphenylsilyl)acetylene for PDI3] were added at room temperature (RT), with a resulting change in color. The reactions continued for 3 days at room conditions, after which PDI1 and PDI2 were obtained in high yields (84 and 93%, respectively) and subsequently

https://doi.org/10.1021/acs.jpcc.1c03131
J. Phys. Chem. C 2021, 125, 13041−13049

purified [column chromatography, chloroform/hexane (1:1 to 1.5:1)]. PDI3 was obtained in 50% yield (silica gel, chloroform/hexane 1:1 to 2:1). The 1,7-isomers of PDI1 and PDI2 were then purified, although the PDI3 isomers could not be purified by column chromatography. As a result, the as-synthesized mixtures of 1,7 and 1,6 isomers of PDIs 1−3 were investigated in this work. Full synthetic details are given in the Supporting Information and Figures S2−S9.

Steady-State Absorption and PL Properties of Dilute Solutions. The absorption and PL spectra of PDIref, PDI1, PDI2, and PDI3 in chloroform ($CHCl_3$, one of the well-known solvents with the best solubility of PDIs) at 10^{-6} M concentration are shown in Figure 2. The high solubility

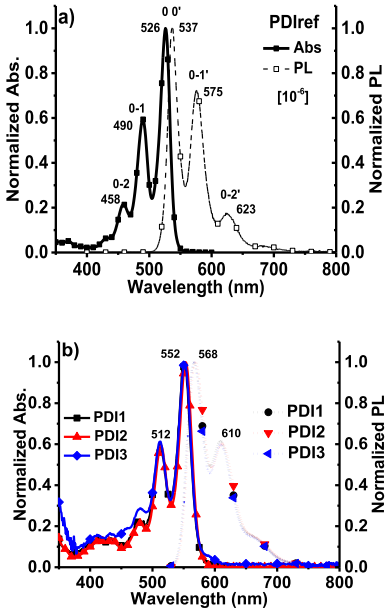

Figure 2. Normalized steady-state absorption and PL of (a) PDIref and (b) PDIs 1−3 in chloroform (10^{-6} M). Excitation wavelengths of PDIref and PDI1−3 are 490 and 512 nm, respectively (i.e., using their 0−1 absorption vibronic bands).

solvent and low concentrations were used to ensure measurements corresponded to isolated molecules. PDIref has an absorption maximum peak ($\pi-\pi^*$) at 526 nm with lower intensity vibronic peaks (S_{0-1} and S_{0-2}) at 490 and 458 nm (Figure 2a). The absorption maximum peak of PDIs 1−3 functionalized with acetylene bridges was 552 nm, redshifted 26 nm compared to PDIref due to their expanded aromatic system. Similar lower intensity vibrational peaks of PDIs 1−3's main absorption were redshifted and found at about 512 (S_{0-1}) and 480 nm (S_{0-2}) (Figure 2b). Molar extinction coefficients were calculated for the main absorbance peak of each material (Figure S10) and were all in the range of 4 to 8 × 10^4 M^{-1} cm^{-1}. PDIs 1−3 exhibited identical maximum PL peak at 568 nm, demonstrating that the silyl group prevents electronic communication between the steric groups and the common core unit.

Electrochemical Properties and Optical Stability. Cyclic voltammetry measurements were carried out to investigate the effect of silane groups on reduction potentials and LUMO levels (Figure 3). While the PDI derivatives did not show any oxidation potential in the positive region, they exhibited double reduction potentials in the negative region as expected.[64] The ethylene bridging group actively participates

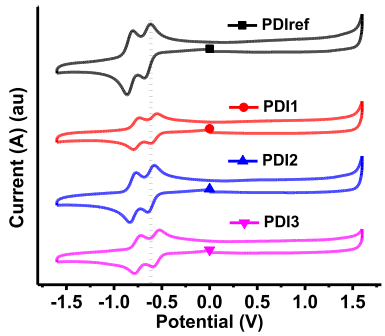

Figure 3. Voltammogram curves of solutions of PDIs with 0.1 M $TBAPF_6$ in dichloromethane.

in the conjugation system and increased the potential of the first half reduction wave compared to PDIref (Table S1). The first half-wave reduction potentials of PDIref, PDI1, PDI2, and PDI3 are −0.61, −0.55, −0.58, and −0.52 V, respectively. The effect of the triphenyl containing silane group in PDI3 was greater than the shift due to the silane groups containing trimethyl and triisopropyl (PDI1 and PDI2) due to the inductively electron-donating phenyl group (Table S1).

The LUMO energy levels of the PDIs were calculated according to the formula $\{E_{LUMO} = -[(E_{red} - E_{Fc}) + 4.8\ eV]\}$ from the 0.45 eV oxidation potential of Fc/Fc^+ and with reference to the vacuum level. Optical band gaps (ΔE_{opt}) were calculated from the energy of the absorption onset. Finally, the HOMO levels were calculated according to the formula "$E_{HOMO} = E_{LUMO} - \Delta E_{opt}$" with all values summarized in Table S1. While PDIref exhibits a band gap of 2.28 eV, PDIs 1−3 exhibit smaller but uniform optical band gaps of around 2.15 eV, consistent with their redshifted but otherwise identical absorption spectra. It is known that sp hybridized groups such as acetylenyl bridges reduce LUMO energy levels and increase the electronegativities of PDIs.[65] The decrease in reduction potentials of PDIs 1−3 substituted by acetylenyl bridges from the bay position showed that the electron affinities increased compared to PDIref. To summarize briefly, they can serve as electron acceptors in organic solar cell applications.

In addition, multicycle CV results of all PDIs demonstrated excellent electrochemically stability (Figure S11). Analogous photostability characterizations were completed by applying continuous excitation for 1 h and monitoring the PL intensity (Figure S12). In both tests, the PDIs were found to be highly stable, a desirable property for their applications in optical−electronic devices. Moreover, the HOMO and LUMO energy levels of the PDIs are compatible with other materials commonly used in optoelectronic devices. This includes hole [e.g., poly(*N*-vinyl carbazole) (PVK) and 4,4′-bis(9-carbazolyl)biphenyl] and electron transport [e.g., (4,6-bis-(3,5-di(pyridin-3-yl)phenyl)-2-methylpyrimidine) B3PYMPM] or host materials (PVK) used in OLEDs.[12,66,67] In addition, these PDIs are likely to be compatible with perovskites or other donor materials in solar cells.[9,10,68]

Time-Resolved PL. The concentration-dependent time-resolved PL behavior of the PDIs (collected with pulsed laser excitation and iCCD camera with gated detection in chloroform solution) is explained in detail in Figures S13−S16 and summarized in Figure 4a−d. Solutions at low and high concentrations reveal the types of excimers and aggregates formed and how these are impacted by the different volumes of protecting silane groups.

https://doi.org/10.1021/acs.jpcc.1c03131
J. Phys. Chem. C 2021, 125, 13041−13049

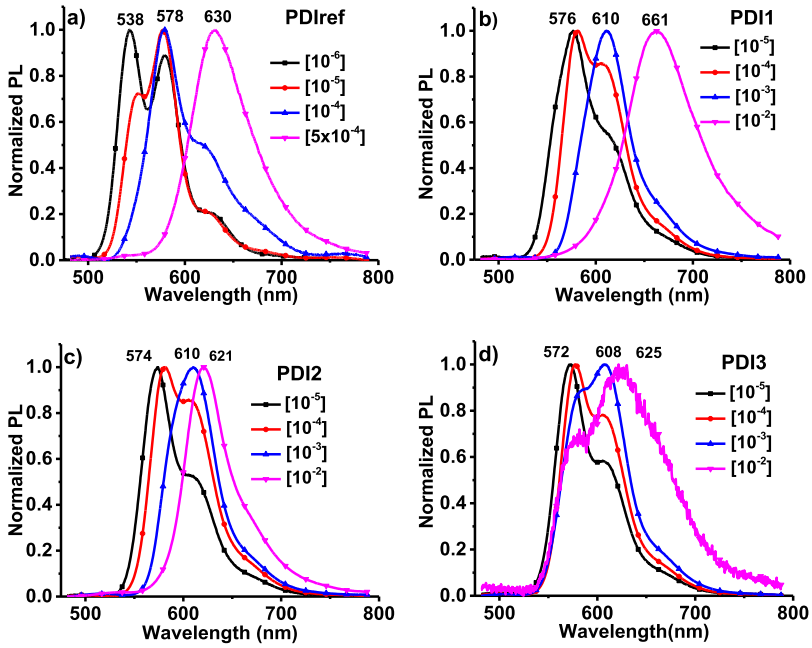

Figure 4. Time-resolved PL spectra at 4.3 ns of PDIref, PDI1, PDI2, and PDI3 at different concentrations in chloroform.

First, PDIref is susceptible to aggregation since it does not have any steric shielding group. When the time-resolved PL spectra of PDIref solutions prepared from concentrations 10^{-6} to 5×10^{-4} M were examined, they exhibited the typical vibrationally resolved emission band ($S_{0-0'}$, $S_{0-1'}$, and $S_{0-2'}$) at low concentrations, consistent with the steady-state spectra (Figure S13a). The PL spectra changes up to a concentration of PDIref 10^{-5} M, with the loss on intensity from the 0−0′ peak likely due to inner filter effects (self-absorption) (Figure S13b). At higher PDIref concentrations (10^{-4} M), the PL peak at 537 nm of monomers disappears, leaving only the lower energy vibronic bands. In addition, a new low-energy aggregate-like emission band appears at 616 nm (Figure S13c). Since no associated change is observed in the absorbance spectrum as the concentration is increased, we attribute this new peak primarily to excimer formation.[29] At the maximum concentration of PDIref, the PL spectrum is of an even lower energy (possibly multimolecular) aggregate-like species, which continued emitting up to 21.7 ns at 629 nm (Figure S13d). The spectra of the new species that are formed depending on concentration are summarized in Figure 4a.

PDI1 exhibited similar concentration-dependent behavior to PDIref (Figure S14a). At 10^{-5} and 10^{-4} M of PDI1, the PL is dominated by the monomeric species with some inner filter effect modulating the PL spectrum shape (Figure S14b). At 10^{-3} and 10^{-2} M, new broad spectra were observed at 632 and 662 nm at longer times (2.2 ns) (Figure S14c,d). As with PDIref, we attribute these to excimer emission and aggregate forms of the PDI1 material. The similarity in behavior of PDIref and PDI1 suggests that the smallest methylsilyl protecting groups do not offer adequate steric bulk to prevent aggregation. What is clear from the time evolution of the emission spectra at high concentrations is that a new long lived emitting species remains after all the monomeric singlet excitons have decayed (Figures S14c,d) showing that the change of the emission band is not simply due to increasing self-absorption at higher concentrations.

PDI2 and PDI3 show similarities in the formation paths of concentration-dependent new PL features species as PDI1, although these do not become apparent until a concentration of 10^{-2} M is reached (Figures S15 and S16). The monomeric emission also persists at higher concentrations in these materials, whereas it becomes fully suppressed in PDIref and PDI1. As the steric shielding groups are larger in PDI2 and PDI3, they are likely more effective at preventing excimer formation at the lower concentrations, with excimer emission only becoming apparent at much higher concentrations. We also do not observe the lowest energy 660 nm excimer band displayed by PDI1 in either PDI2 or PDI3 at the investigated concentrations, consistent with their steric shielding preventing the formation of higher-order aggregates.

Concentration-Dependent PLQY Measurements. ACQ effects of silylethynyl substitution on PDIs were also investigated by concentration-dependent PLQY measurements (absolute method in integrating sphere). The excitation wavelengths were 490 nm for PDIref and 512 nm for PDIs 1−3 (Figure S17 and TOC graphic). All PDI derivatives exhibited Φs > 90% and above up to 10^{-4} M, indicating high efficiency for isolated molecules. At 10^{-3} M concentration, PDIref and PDI1 suffer significant ACQ due to the formation of aggregates and excimers identified by time-resolved PL, with Φ decreasing to ∼60%. More shielded PDI2 and PDI3 are not as affected, showing resistance to aggregation at these concentrations and retaining PLQYs above 85%. At a very high concentration of 10^{-2} M, the steric shielding of PDI2 and PDI3 still performed quite effectively, retaining Φ values of 67 and 58%, respectively. In contrast, PDIref was insoluble at 10 mM, while PDI1 at this concentration gave Φ of only 22%. Interestingly, from these results, we note that the shielding performance of PDI2 and PDI3 is very similar. This indicates that the larger triphenyl shielding offers no additional benefits compared to triisopropyl groups.

Investigating this steric protection in the extreme limit, PLQYs of neat films were also investigated—prepared by spin coating (for PDIs 1−3; 2500 rpm, 10 mg/mL) (for PDIref;

https://doi.org/10.1021/acs.jpcc.1c03131
J. Phys. Chem. C 2021, 125, 13041−13049

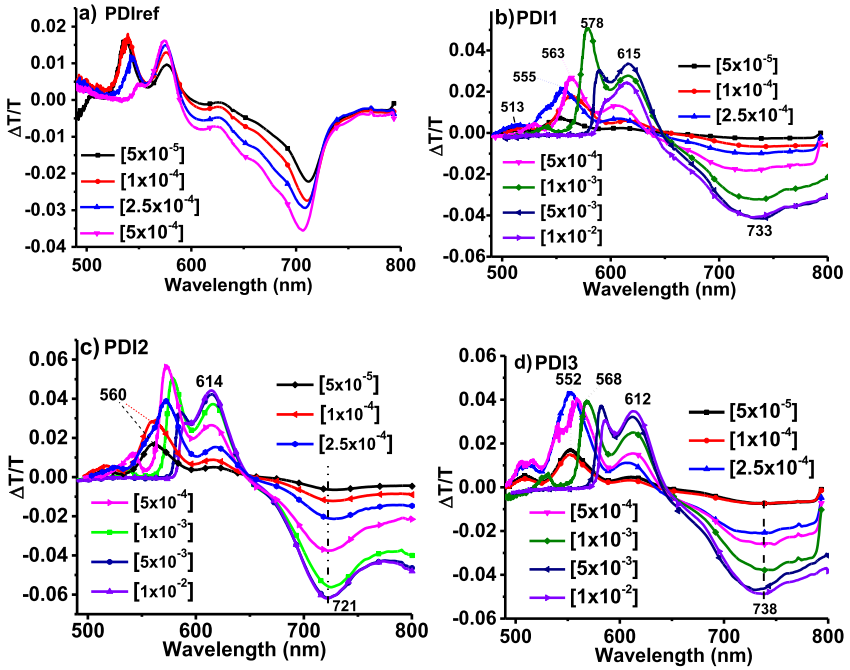

Figure 5. TAS curves of PDIref and PDIs 1−3 at different concentrations in chloroform (80 ps delayed time).

2500 rpm, 5 mg/mL). PDIref and PDI1 exhibited PLQYs of only 2.1 and 2.4%, respectively, in the neat films. More protected PDI2 and PDI3 instead gave 16.8 and 15%, respectively. The PLQYs of the films clearly decreased compared to the solution phase as the total removal of solvent strongly promotes molecular aggregation and excimer formation. The formation of such multimolecular states is apparent from the change in absorption and PL spectra displayed by the neat films (Figure S18), although with PDI2 and PDI3 less severely affected. Almost total ACQ was observed in PDIref and PDI1 due to the lack of effective steric protection and thus their potential to form closely spaced coplanar structures.[19] The more substantial steric shielding in PDI2 and PDI3 prevents this interaction, allowing them to retain higher PLQYs in the neat films. The fact that the triisopropylsilane and triphenylsilane groups result in similar outcomes for these two materials (as was observed in solution measurements) demonstrates that they have reached the limit of diminishing returns as it concerns protecting group size and prevention of ACQ. Although these neat film PLQYs are lower than what can typically be achieved by embedding the material in an optically transparent host,[56] such values can still be suitable for applications as emitters in high-luminance OLEDs, with the enhanced solubility of the PDIs potentially supporting improved solution-processing applications.[69,70]

Femtosecond-TAS (fs-TAS) Properties of PDIs. TAS measurements of different concentration chloroform solutions of the PDIs were performed in the 480−800 nm range. Part of the 1030 nm output from the femtosecond amplifier PHAROS was used to generate 343 nm via third harmonic generation, which is used as the pump to excite the PDIs. Another part of the 1030 nm output was focused on a 2 mm sapphire plate to generate white light continuum, which was used as a probe to observe the excited-state behavior. More detailed information about the pump−probe fs-TAS technique is detailed in the Supporting Information.

The induced absorption spectra of each PDI at 80 ps delayed time are summarized in Figure 5. TAS measurements of PDI solutions at 5×10^{-5} to 5×10^{-4} M showed only singlet-state dynamics. The PDIref at 5×10^{-5} M exhibited ground-state bleach (GSB) and stimulated emission (SE) signals at 537 nm and also SE of the $S_{0-1'}$ fluorescence transition at 574 nm, following the steady-state and 2 ns time-resolved PL spectra as a function of concentration extremely closely. A photoinduced absorption (PIA) peak of PDIref was seen at 711 nm (Figure 5a), which likely corresponds to S_1 to S_2 absorption. Changes in TAS spectra were observed with a controlled increase in the PDIref concentration. The intensity of the SE at 537 nm decreased (likely due to inner filter effects and increased self-absorption), while the SE at 574 nm increased its intensity due to increased pump beam absorption in the sample. In the PIA region, shifts to short wavelengths of a few nanometer were detected and exhibited PIA with a maximum peak at 706 nm at 5×10^{-4} M (Figure 5a). Throughout the TAS measurements, we observe no indication of the formation of triplet states, which is consistent with low intersystem crossing in these materials and their high intrinsic PLQYs. More importantly, we also do not observe the appearance of a new instantaneous PIA feature at high concentrations that could be associated with states resulting from ground-state interactions such as dimers and small aggregates. This further points to the main intermolecular interaction at high concentrations being excimeric in nature.

The concentration-dependent TAS spectra of PDIs 1−3 are illustrated in Figure 5b−d (at 80 ps). Although this delay time is before the emergence of excimer PL from the time-resolved emission measurements, no further change in the TAS spectral shape was observed at any other time for any material at any concentration, up to ∼5 ns for these measurements (Figure S19). Since the solubilities of PDIs 1−3 were higher, measurements were also completed at higher concentrations such as 10^{-2} M. PDI1 exhibits longer wavelength GSB and SE due to extension of its aromatic system with the ethynyl

https://doi.org/10.1021/acs.jpcc.1c03131
J. Phys. Chem. C 2021, 125, 13041−13049

bridges in line with the steady-state measurements, found at 515 nm (GSB), 555 nm (GSB), 578 nm (SE), and 615 nm (SE), respectively (at 5×10^{-5} M). At higher concentrations the GSB was not always observed due to the high absorption, while SE was evident at 578 and 615 nm at 10^{-3} M. The PIA peak at all concentrations was determined to be about 733 nm (Figure 5b). PDI2 and PDI3 exhibited similar TAS properties as PDI1, confirming their similar optoelectronic properties but revealing little about the aggregate or excimer state from the available range of wavelengths and timescales (Figure 5c).

Excited-state lifetimes of PDIs 1−3 were determined by exponential fitting of the TAS signal decay (amplitude weighted average of biexponential fit). The excited-state lifetime of PDI1, 2, and 3 at 10^{-4} M were 4.4, 5.2, and 12.2 ns, respectively, although we suggest that the value for PDI3 may be an outlier due to low optical density at this concentration. At 10^{-3} M concentrations, the lifetimes increased to 7.4 and 7.58 ns for PDI1 and PDI2, while for PDI3, it appeared to decrease to 8.5 ns (Table S3). These excited-state lifetimes were also comparable with the ∼8 ns lifetimes observed for the emission decays if PDIs 1−3 (Figures S20−S22) with a longer-lived component emerging at higher concentrations attributed to excimer emission.

Finally, we note that the best PLQY values we are able to achieve in the neat film (15 and 17%) are significantly lower than some recently reported values using dendritic ether-bridged PDI bay substituents (up to 60% PLQY or 90% in crystals[44,49]). Nonetheless, the use of electronically insulating silyl groups is able to fully decouple the electronic systems of the PDI core and the shielding groups. This leads to more stable absorption and emission spectra as the shielding group size increases. Our PLQYs are instead similar to those achieved using dendritic steric groups attached to the imide position (21 and 29%[1]).

The different PLQY values achieved with these shielding strategies are likely due to the different structural shapes associated with each. X-ray analysis shows that dendritic ether-linked shielding groups at the bay positions are able to wrap around the PDI core and provide 360-degree protection.[44] The very similar shielding groups employed at the imide position are able to protect the plane of the PDI core from above and below but not as effectively from the side.[1] This difference probably accounts for the differences in neat-film PLQYs reported in those two studies. The ethynyl−silyl groups here are instead expected to provide dumbbell-like protuberances, preventing other molecules from approaching in the plane of the PDI core but not perpendicular to it—completely in contrast to the imide-substituent strategy. Clearly, the fully enwrapped PDI is the most resilient to ACQ, although alternate shielding strategies such as the one presented here may prove to be more effective at preserving the electronic properties of PDI, which would likely be disrupted by the same shielding that protects against ACQ. The directionality of the shielding strategy is also likely to be critical in surface-bound applications, where ACQ and excimer formation happen at predictable molecular geometries.[28]

CONCLUSIONS

Due to the large planar aromatic systems of PDIs, they are prone to form aggregates and dimers or excimers at high concentrations that negatively impact their optoelectronic performance. In this study, we have synthesized three different silylethynyl-substituted PDIs to investigate the effects of their differently sized silane groups relevant to ACQ and aggregation behavior. PDI1, 2, and 3 exhibited the same photophysical properties at low concentrations, while the larger volumes of silane groups bestowed PDI2 and PDI3 with greater solubility and resistance to excimer formation than PDI1 (with smaller steric groups) and PDIref (with no protection). Time-resolved PL measurements revealed the formation of excimers or multimolecular aggregates, which PDI2 and PDI3 are not susceptible to even at very high concentrations. Steady-state and transient absorption measurements further establish the formation of excimer species rather than ground-state dimers. Both PDI3 and PDI2 consequently retain high PLQYs even at very high concentrations and retain more of this performance in neat films compared to PDIref and PDI1. This strategy for preventing aggregation formation therefore has the potential to be applied for a wide range of organic electronic materials that suffer aggregation effects at high concentrations.

ASSOCIATED CONTENT

Supporting Information

The Supporting Information is available free of charge at https://pubs.acs.org/doi/10.1021/acs.jpcc.1c03131.

Synthesis of PDIs and their structural, electrochemical, and optical characterizations; additional time-resolved emission and transient absorption spectra; PLQY data and optical spectra of neat films; and decay fitting of time-resolved emission and transient absorption signal decays (PDF)

AUTHOR INFORMATION

Corresponding Authors

Erkan Aksoy − *Solar Energy Institute, Ege University, 35100 Izmir, Turkey; Department of Physics, Durham University, Durham DH1 3LE, U.K.; Department of Photonics, Izmir Institute of Technology, 35430 Urla, Izmir, Turkey;* orcid.org/0000-0002-0083-2574; Email: erkanaksoy@iyte.edu.tr

Andrew P. Monkman − *Department of Physics, Durham University, Durham DH1 3LE, U.K.;* orcid.org/0000-0002-0784-8640; Email: a.p.monkman@durham.ac.uk

Authors

Andrew Danos − *Department of Physics, Durham University, Durham DH1 3LE, U.K.;* orcid.org/0000-0002-1752-8675

Chunyong Li − *Department of Physics, Durham University, Durham DH1 3LE, U.K.*

Canan Varlikli − *Department of Photonics, Izmir Institute of Technology, 35430 Urla, Izmir, Turkey;* orcid.org/0000-0002-1081-0803

Complete contact information is available at: https://pubs.acs.org/10.1021/acs.jpcc.1c03131

Notes

The authors declare no competing financial interest.

ACKNOWLEDGMENTS

E.A. thanks The Scientific and Technological Research Council of Turkey (TUBITAK) BIDEB-2214-A (Appl. # 1059B141800476) who supported this research financially—for time-resolved PL and ultrafast pump−probe TAS. E.A. and C.V. also thank the project support funds of TUBITAK (grant

#119F031) for financial support of the synthesis, structural, electrochemical, and optical characterizations of perylene derivatives. A.D. and A.P.M. were supported by the Hyper-OLED project from the European Unions's Horizon 2020 Research and Innovation Program under grant agreement number 732013.

REFERENCES

(1) Zhang, B.; Soleimaninejad, H.; Jones, D. J.; White, J. M.; Ghiggino, K. P.; Smith, T. a.; Wong, W. W. H. Highly Fluorescent Molecularly Insulated Perylene Diimides: Effect of Concentration on Photophysical Properties. *Chem. Mater.* **2017**, *29*, 8395−8403.
(2) Würthner, F.; Saha-Möller, C. R.; Fimmel, B.; Ogi, S.; Leowanawat, P.; Schmidt, D. Perylene Bisimide Dye Assemblies as Archetype Functional Supramolecular Materials. *Chem. Rev.* **2016**, *116*, 962−1052.
(3) Huang, C.; Barlow, S.; Marder, S. R. Perylene-3,4,9,10-Tetracarboxylic Acid Diimides: Synthesis, Physical Properties, and Use in Organic Electronics. *J. Org. Chem.* **2011**, *76*, 2386−2407.
(4) Guner, T.; Aksoy, E.; Demir, M. M.; Varlikli, C. Perylene-Embedded Electrospun PS Fibers for White Light Generation. *Dyes Pigm.* **2019**, *160*, 501−508.
(5) Karapire, C.; Zafer, C.; İçli, S. Studies on Photophysical and Electrochemical Properties of Synthesized Hydroxy Perylenediimides in Nanostructured Titania Thin Films. *Synth. Met.* **2004**, *145*, 51−60.
(6) Kus, M.; Hakli, Ö.; Zafer, C.; Varlikli, C.; Demic, S.; Özçelik, S.; Icli, S. Optical and Electrochemical Properties of Polyether Derivatives of Perylenediimides Adsorbed on Nanocrystalline Metal Oxide Films. *Org. Electron.* **2008**, *9*, 757−766.
(7) Karapire, C.; Kus, M.; Turkmen, G.; Trevithick-Sutton, C. C.; Foote, C. S.; Icli, S. Photooxidation Studies with Perylenediimides in Solution, PVC and Sol-Gel Thin Films under Concentrated Sun Light. *Sol. Energy* **2005**, *78*, 5−17.
(8) Bozkus, V.; Aksoy, E.; Varlikli, C. Perylene Based Solution Processed Single Layer Woled with Adjustable CCT and CRI. *Electron* **2021**, *10*, 725.
(9) Yan, W.; He, Z.; Jiang, J.; Lu, D.; Gong, Y.; Yang, W.; Xia, R.; Huang, W.; Xin, H. Highly Thermal-Stable Perylene-Bisimide Small Molecules as Efficient Electron-Transport Materials for Perovskite Solar Cells. *J. Mater. Chem. C* **2020**, *8*, 14773−14781.
(10) Chen, W.; Yang, X.; Long, G.; Wan, X.; Chen, Y.; Zhang, Q. A Perylene Diimide (PDI)-Based Small Molecule with Tetrahedral Configuration as a Non-Fullerene Acceptor for Organic Solar Cells. *J. Mater. Chem. C* **2015**, *3*, 4698−4705.
(11) Liu, M.; Wang, H.; Tang, Q.; Zhao, X.; Tong, Y.; Liu, Y. Ultrathin Air-Stable N-Type Organic Phototransistor Array for Conformal Optoelectronics. *Sci. Rep.* **2018**, *8*, 1−10.
(12) Kozma, E.; Mróz, W.; Villafiorita-Monteleone, F.; Galeotti, F.; Andicsová-Eckstein, A.; Catellani, M.; Botta, C. Perylene Diimide Derivatives as Red and Deep Red-Emitters for Fully Solution Processable OLEDs. *RSC Adv.* **2016**, *6*, 61175−61179.
(13) Zafer, C.; Karapire, C.; Serdar Sariciftci, N.; Icli, S.; Serdar Sariciftci, N.; Icli, S. Characterization of N, N′-Bis-2-(1-Hydoxy-4-Methylpentyl)-3, 4, 9, 10-Perylene Bis (dicarboximide) Sensitized Nanocrystalline TiO2 Solar Cells with Polythiophene Hole Conductors. *Sol. Energy Mater. Sol. Cells* **2005**, *88*, 11−21.
(14) Aksoy, E.; Demir, N.; Varlikli, C. White LED Light Production Using Dibromoperylene Derivatives in down Conversion of Energy. *Can. J. Phys.* **2018**, *96*, 734−739.
(15) Kozma, E.; Mróz, W.; Galeotti, F. A Polystyrene Bearing Perylene Diimide Pendants with Enhanced Solid State Emission for White Hybrid Light-Emitting Diodes. *Dyes Pigm.* **2015**, *114*, 138−143.
(16) Banal, J. L.; Soleimaninejad, H.; Jradi, F. M.; Liu, M.; White, J. M.; Blakers, A. W.; Cooper, M. W.; Jones, D. J.; Ghiggino, K. P.; Marder, S. R.; et al. Energy Migration in Organic Solar Concentrators with a Molecularly Insulated Perylene Diimide. *J. Phys. Chem. C* **2016**, *120*, 12952−12958.
(17) Sanguineti, A.; Sassi, M.; Turrisi, R.; Ruffo, R.; Vaccaro, G.; Meinardi, F.; Beverina, L. High Stokes Shift Perylene Dyes for Luminescent Solar Concentrators. *Chem. Commun.* **2013**, *49*, 1618−1620.
(18) Davis, N. J. L. K.; Macqueen, R. W.; Roberts, D. a.; Danos, A.; Dehn, S.; Perrier, S.; Schmidt, T. W. Energy Transfer in Pendant Perylene Diimide Copolymers. *J. Mater. Chem. C* **2016**, *4*, 8270−8275.
(19) Brown, K. E.; Salamant, W. A.; Shoer, L. E.; Young, R. M.; Wasielewski, M. R. Direct Observation of Ultrafast Excimer Formation in Covalent Perylenediimide Dimers Using near-Infrared Transient Absorption Spectroscopy. *J. Phys. Chem. Lett.* **2014**, *5*, 2588−2593.
(20) Zong, L.; Zhang, H.; Li, Y.; Gong, Y.; Li, D.; Wang, J.; Wang, Z.; Xie, Y.; Han, M.; Peng, Q.; et al. Tunable Aggregation-Induced Emission Nanoparticles by Varying Isolation Groups in Perylene Diimide Derivatives and Application in Three-Photon Fluorescence Bioimaging. *ACS Nano* **2018**, *12*, 9532−9540.
(21) Ye, C.; Gray, V.; Kushwaha, K.; Kumar Singh, S.; Erhart, P.; Börjesson, K. Optimizing Photon Upconversion by Decoupling Excimer Formation and Triplet Triplet Annihilation. *Phys. Chem. Chem. Phys.* **2020**, *22*, 1715−1720.
(22) Ye, C.; Gray, V.; Mårtensson, J.; Börjesson, K. Annihilation Versus Excimer Formation by the Triplet Pair in Triplet-Triplet Annihilation Photon Upconversion. *J. Am. Chem. Soc.* **2019**, *141*, 9578−9584.
(23) Danos, A.; MacQueen, R. W.; Cheng, Y. Y.; Dvořák, M.; Darwish, T. a.; McCamey, D. R.; Schmidt, T. W. Deuteration of Perylene Enhances Photochemical Upconversion Efficiency. *J. Phys. Chem. Lett.* **2015**, *6*, 3061−3066.
(24) McHale, J. L. Hierarchal Light-Harvesting Aggregates and Their Potential for Solar Energy Applications. *J. Phys. Chem. Lett.* **2012**, *3*, 587−597.
(25) Fink, R. F.; Seibt, J.; Engel, V.; Renz, M.; Kaupp, M.; Lochbrunner, S.; Zhao, H.-M.; Pfister, J.; Würthner, F.; Engels, B. Exciton Trapping in Π-Conjugated Materials: A Quantum-Chemistry-Based Protocol Applied to Perylene Bisimide Dye Aggregates. *J. Am. Chem. Soc.* **2008**, *130*, 12858−12859.
(26) Etherington, M. K.; Kukhta, N. a.; Higginbotham, H. F.; Danos, A.; Bismillah, A. N.; Graves, D. R.; McGonigal, P. R.; Haase, N.; Morherr, A.; Batsanov, A. S.; Pflumm, C.; et al. Persistent Dimer Emission in Thermally Activated Delayed Fluorescence Materials. *J. Phys. Chem. C* **2019**, *123*, 11109−11117.
(27) Salah, L.; Etherington, M. K.; Shuaib, A.; Danos, A.; Nazeer, A. a.; Ghazal, B.; Prlj, A.; Turley, A. T.; Mallick, A.; McGonigal, P. R.; et al. Suppressing Dimer Formation by Increasing Conformational Freedom in Multi-Carbazole Thermally Activated Delayed Fluorescence Emitters. *J. Mater. Chem. C* **2021**, *9*, 189−198.
(28) Gorman, J.; Pandya, R.; Allardice, J. R.; Price, M. B.; Schmidt, T. W.; Friend, R. H.; Rao, A.; Davis, N. J. L. K. Excimer Formation in Carboxylic Acid-Functionalized Perylene Diimides Attached to Silicon Dioxide Nanoparticles. *J. Phys. Chem. C* **2019**, *123*, 3433−3440.
(29) Stavrou, K.; Danos, A.; Hama, T.; Hatakeyama, T.; Monkman, A. Hot Vibrational States in a High-Performance Multiple Resonance Emitter and the Effect of Excimer Quenching on Organic Light-Emitting Diodes. *ACS Appl. Mater. Interfaces* **2021**, *13*, 8643−8655.
(30) Howard, I. A.; Laquai, F.; Keivanidis, P. E.; Friend, R. H.; Greenham, N. C. Perylene Tetracarboxydiimide as an Electron Acceptor in Organic Solar Cells: A Study of Charge Generation and Recombination. *J. Phys. Chem. C* **2009**, *113*, 21225−21232.
(31) Lim, J. M.; Kim, P.; Yoon, M.-C.; Sung, J.; Dehm, V.; Chen, Z.; Würthner, F.; Kim, D. Exciton Delocalization and Dynamics in Helical Π-Stacks of Self-Assembled Perylene Bisimides. *Chem. Sci.* **2013**, *4*, 388−397.
(32) Sadiq, F.; Wang, Z.; Hou, Y.; Zhao, J.; Elmali, A.; Escudero, D.; Karatay, A. Thienyl/phenyl Bay-Substituted Perylenebisimides: Intersystem Crossing and Application as Heavy Atom-Free Triplet Photosensitizers. *Dyes Pigm.* **2021**, *184*, 108708.

https://doi.org/10.1021/acs.jpcc.1c03131
J. Phys. Chem. C 2021, 125, 13041−13049

(33) Son, M.; Park, K. H.; Shao, C.; Würthner, F.; Kim, D. Spectroscopic Demonstration of Exciton Dynamics and Excimer Formation in a Sterically Controlled Perylene Bisimide Dimer Aggregate. *J. Phys. Chem. Lett.* **2014**, *5*, 3601−3607.
(34) Inci, M. N.; Acikgoz, S.; Demir, M. M. Monitoring Excimer Formation of Perylene Dye Molecules within PMMA-Based Nanofiber via FLIM Method. *Nanophotonics* **2016**, *9884*, 988413.
(35) Ferreira, J. a.; Porter, G. Concentration Quenching and Excimer Formation by Perylene in Rigid Solutions. *J. Chem. Soc., Faraday Trans. 2* **1977**, *73*, 340−348.
(36) Piosik, E.; Synak, A.; Paluszkiewicz, J.; Martyński, T. Concentration Dependent Evolution of Aggregates Formed by Chlorinated and Non-Chlorinated Perylene Tetracarboxylic Acid Esters in Pure Spin-Coated Films and in a PMMA Matrix. *J. Lumin.* **2019**, *206*, 132−145.
(37) Rossi, A.; Price, M. B.; Hardy, J.; Gorman, J.; Schmidt, T. W.; Davis, N. J. L. K. Energy Transfer between Perylene Diimide Based Ligands and Cesium Lead Bromide Perovskite Nanocrystals. *J. Phys. Chem. C* **2020**, *124*, 3306−3313.
(38) Price, M. B.; Paton, A.; Gorman, J.; Wagner, I.; Laufersky, G.; Chen, K.; Friend, R. H.; Schmidt, T. W.; Hodgkiss, J. M.; Davis, N. J. L. K. Inter-Ligand Energy Transfer in Dye Chromophores Attached to High Bandgap SiO2 Nanoparticles. *Chem. Commun.* **2019**, *55*, 8804−8807.
(39) Congrave, D. G.; Drummond, B. H.; Gray, V.; Bond, A. D.; Rao, A.; Friend, R. H.; Bronstein, H. Suppressing Aggregation Induced Quenching in Anthracene Based Conjugated Polymers. *Polym. Chem.* **2021**, *12*, 1830−1836.
(40) Cho, H. J.; Kim, S. W.; Kim, S.; Lee, S.; Lee, J.; Cho, Y.; Lee, Y.; Lee, T.-W.; Shin, H.-J.; Song, C. Suppressing Π−π Stacking Interactions for Enhanced Solid-State Emission of Flat Aromatic Molecules via Edge Functionalization with Picket-Fence-Type Groups. *J. Mater. Chem. C* **2020**, *8*, 17289.
(41) Royakkers, J.; Minotto, A.; Congrave, D. G.; Zeng, W.; Patel, A.; Bond, A. D.; Bučar, D.-K.; Cacialli, F.; Bronstein, H. Doubly Encapsulated Perylene Diimides: Effect of Molecular Encapsulation on Photophysical Properties. *J. Org. Chem.* **2020**, *85*, 207−214.
(42) Fujiwara, Y.; Ozawa, R.; Onuma, D.; Suzuki, K.; Yoza, K.; Kobayashi, K. Double Alkylene-Strapped Diphenylanthracene as a Photostable and Intense Solid-State Blue-Emitting Material. *J. Org. Chem.* **2013**, *78*, 2206−2212.
(43) Royakkers, J.; Minotto, A.; Congrave, D. G.; Zeng, W.; Hassan, A.; Leventis, A.; Cacialli, F.; Bronstein, H. Suppressing Solid-State Quenching in Red-Emitting Conjugated Polymers. *Chem. Mater.* **2020**, *32*, 10140−10145.
(44) Schmidt, D.; Stolte, M.; Süß, J.; Liess, A.; Stepanenko, V.; Würthner, F. Protein-like Enwrapped Perylene Bisimide Chromophore as a Bright Microcrystalline Emitter Material. *Angew. Chem., Int. Ed.* **2019**, *58*, 13385−13389.
(45) Görl, D.; Zhang, X.; Stepanenko, V.; Würthner, F. Supramolecular Block Copolymers by Kinetically Controlled Co-Self-Assembly of Planar and Core-Twisted Perylene Bisimides. *Nat. Commun.* **2015**, *6*, 1−8.
(46) Aksakal, N. E.; Chumakov, Y.; Yuksel, F. Crystal Structures of Two Perylenediimides: A Study of Bay-Substitution. *J. Chem. Crystallogr.* **2019**, *49*, 72−79.
(47) Dubey, R. K.; Eustace, S. J.; Van Mullem, J. S.; Sudhölter, E. J. R.; Grozema, F. C.; Jager, W. F. Perylene Bisimide Dyes with up to Five Independently Introduced Substituents: Controlling the Functionalization Pattern and Photophysical Properties Using Regiospecific Bay Substitution. *J. Org. Chem.* **2019**, *84*, 9532−9547.
(48) Inan, D.; Dubey, R. K.; Westerveld, N.; Bleeker, J.; Jager, W. F.; Grozema, F. C. Substitution Effects on the Photoinduced Charge-Transfer Properties of Novel Perylene-3,4,9,10-Tetracarboxylic Acid Derivatives. *J. Phys. Chem. A* **2017**, *121*, 4633−4644.
(49) Stolte, M.; Schembri, T.; Süß, J.; Schmidt, D.; Krause, A.-M.; Vysotsky, M. O.; Würthner, F. 1-Mono- and 1,7-Disubstituted Perylene Bisimide Dyes with Voluminous Groups at Bay Positions: In Search for Highly Effective Solid-State Fluorescence Materials. *Chem. Mater.* **2020**, *32*, 6222−6236.
(50) Yang, J.; Chen, F.; Cong, P.; Xiao, H.; Geng, Y.; Liao, Z.; Chen, L.; Zhang, B.; Zhou, E. Tuning the Optoelectronic Properties of Vinylene Linked Perylenediimide Dimer by Ring Annulation at the inside or Outside Bay Positions for Fullerene-Free Organic Solar Cells. *J. Energy Chem.* **2020**, *40*, 112−119.
(51) Meng, D.; Sun, D.; Zhong, C.; Liu, T.; Fan, B.; Huo, L.; Li, Y.; Jiang, W.; Choi, H.; Kim, T.; et al. High-Performance Solution-Processed Non-Fullerene Organic Solar Cells Based on Selenophene-Containing Perylene Bisimide Acceptor. *J. Am. Chem. Soc.* **2016**, *138*, 375−380.
(52) Colella, M.; Danos, A.; Monkman, A. P. Less Is More: Dilution Enhances Optical and Electrical Performance of a TADF Exciplex. *J. Phys. Chem. Lett.* **2019**, *10*, 793−798.
(53) Colella, M.; Danos, A.; Monkman, A. P. Identifying the Factors That Lead to PLQY Enhancement in Diluted TADF Exciplexes Based on Carbazole Donors. *J. Phys. Chem. C* **2019**, *123*, 17318−17324.
(54) Xiong, Y.; Wu, B.; Zheng, X.; Zhao, Z.; Deng, P.; Lin, M.; Tang, B.; Ong, B. S. Novel Dimethylmethylene-Bridged Triphenylamine-PDI Acceptor for Bulk-Heterojunction Organic Solar Cells. *Adv. Sci.* **2017**, *4*, 1700110.
(55) Bian, G.-F.; Zhao, F.; Lau, T.-K.; Sheng, C.-Q.; Lu, X.; Du, H.; Zhang, C.; Qu, Z.-R.; Chen, H.; Wan, J.-H. Simply Planarizing Nonfused Perylene Diimide Based Acceptors toward Promising Non-Fullerene Solar Cells. *J. Mater. Chem. C* **2019**, *7*, 8092−8100.
(56) Aksoy, E.; Danos, A.; Varlikli, C.; Monkman, A. P. Navigating CIE Space for Efficient TADF Downconversion WOLEDs. *Dyes Pigm.* **2020**, *183*, 108707.
(57) Chen, S.; Liu, Y.; Qiu, W.; Sun, X.; Ma, Y.; Zhu, D. Oligothiophene-Functionalized Perylene Bisimide System: Synthesis, Characterization, and Electrochemical Polymerization Properties. *Chem. Mater.* **2005**, *17*, 2208−2215.
(58) Jiménez, Á. J.; Spänig, F.; Rodríguez-Morgade, M. S.; Ohkubo, K.; Fukuzumi, S.; Guldi, D. M.; Torres, T. A Tightly Coupled Bis(zinc(ll) Phthalocyanine)-Perylenediimide Ensemble to Yield Long-Lived Radical Ion Pair States. *Org. Lett.* **2007**, *9*, 2481−2484.
(59) Pettipas, R. D.; Radford, C. L.; Kelly, T. L. Regioisomerically Pure 1,7-Dicyanoperylene Diimide Dimer for Charge Extraction from Donors with High Electron Affinities. *ACS Omega* **2020**, *5*, 16547−16555.
(60) Sengupta, S.; Dubey, R. K.; Hoek, R. W. M.; Van Eeden, S. P. P.; Gunbaş, D. D.; Grozema, F. C.; Sudhölter, E. J. R.; Jager, W. F. Synthesis of Regioisomerically Pure 1,7-Dibromoperylene-3,4,9,10-tetracarboxylic Acid Derivatives. *J. Org. Chem.* **2014**, *79*, 6655−6662.
(61) Rajasingh, P.; Cohen, R.; Shirman, E.; Shimon, L. J. W.; Rybtchinski, B. Selective Bromination of Perylene Diimides under Mild Conditions. *J. Org. Chem.* **2007**, *72*, 5973−5979.
(62) Ma, J.; Yin, L.; Zou, G.; Zhang, Q. Regioisomerically Pure 1,7-Dibromo-Substituted Perylene Bisimide Dyes: Efficient Synthesis, Separation, and Characterization. *Eur. J. Org. Chem.* **2015**, *2015*, 3296−3302.
(63) Zeng, C.; Meng, D.; Jiang, W.; Wang, Z. Synthesis of Isomeric Perylenodithiophene Diimides. *Org. Lett.* **2018**, *20*, 6606−6609.
(64) Oner, I.; Varlikli, C.; Icli, S. The Use of a Perylenediimide Derivative as a Dopant in Hole Transport Layer of an Organic Light Emitting Device. *Appl. Surf. Sci.* **2011**, *257*, 6089−6094.
(65) Yan, Q.; Zhao, D. Conjugated Dimeric and Trimeric Perylenediimide Oligomers. *Org. Lett.* **2009**, *11*, 3426−3429.
(66) Yen, J.-H.; Wang, Y.-J.; Hsieh, C.-A.; Chen, Y.-C.; Chen, L.-Y. Enhanced Light Extraction from Organic Light-Emitting Devices through Non-Covalent or Covalent Polyimide-Silica Light Scattered Hybrid Films. *J. Mater. Chem. C* **2020**, *8*, 4102.
(67) Wen, L.; Li, F.; Xie, J.; Wu, C.; Zheng, Y.; Chen, D.; Xu, S.; Guo, T.; Qu, B.; Chen, Z.; et al. Electroplex Emission at PVK/Bphen Interface for Application in White Organic Light-Emitting Diodes. *J. Lumin.* **2011**, *131*, 2252−2254.
(68) Zheng, M.; Miao, Y.; Syed, A. A.; Chen, C.; Yang, X.; Ding, L.; Li, H.; Cheng, M. Spatial Configuration Engineering of Perylenedii-

mide-Based Non-Fullerene Electron Transport Materials for Efficient Inverted Perovskite Solar Cells. *J. Energy Chem.* **2021**, *56*, 374−382.
(69) Keum, C.; Becker, D.; Archer, E.; Bock, H.; Kitzerow, H.; Gather, M. C.; Murawski, C. Organic Light-Emitting Diodes Based on a Columnar Liquid-Crystalline Perylene Emitter. *Adv. Opt. Mater.* **2020**, *8*, 2000414.
(70) Dayneko, S. V.; Rahmati, M.; Pahlevani, M.; Welch, G. C. Solution Processed Red Organic Light-Emitting-Diodes Using an: N-Annulated Perylene Diimide Fluorophore. *J. Mater. Chem. C* **2020**, *8*, 2314−2319.

https://doi.org/10.1021/acs.jpcc.1c03131
J. Phys. Chem. C 2021, 125, 13041−13049